

# Electrosurgery With Cellular Precision

Daniel V. Palanker\*, Alexander Vankov, and Philip Huie

**Abstract**—Electrosurgery, one of the most-often used surgical tools, is a robust but somewhat crude technology that has changed surprisingly little since its invention almost a century ago. Continuous radiofrequency is still used for tissue cutting, with thermal damage extending to hundreds of micrometers. In contrast, lasers developed 70 years later, have been constantly perfected, and the laser-tissue interactions explored in great detail, which has allowed tissue ablation with cellular precision in many laser applications. We discuss mechanisms of tissue damage by electric field, and demonstrate that electrosurgery with properly optimized waveforms and microelectrodes can rival many advanced lasers. Pulsed electric waveforms with burst durations ranging from 10 to 100  $\mu\text{s}$  applied via insulated planar electrodes with 12  $\mu\text{m}$  wide exposed edges produced plasma-mediated dissection of tissues with the collateral damage zone ranging from 2 to 10  $\mu\text{m}$ . Length of the electrodes can vary from micrometers to centimeters and all types of soft tissues—from membranes to cartilage and skin could be dissected in liquid medium and in a dry field. This technology may allow for major improvements in outcomes of the current surgical procedures and development of much more refined surgical techniques.

**Index Terms**—Cavitation, electrosurgery, electroporation, pulsed ablation, thermal confinement.

## I. INTRODUCTION

ELECTROSURGERY was invented in the beginning of the 20th century [1] and became one of the most basic “work horse” surgical technologies after Bovie introduced his radiofrequency (RF) generator in 1926 [2]. A measure of the broad acceptance of electrosurgical technology in medicine is reflected in the very large size of its market—in excess of \$1 billion in 2006. Fundamentals of electrosurgery have not changed much since the Bovie generator—cutting is performed using continuous RF waveform, which thermally ablates soft tissue leaving a collateral damage zone of 100–400  $\mu\text{m}$  [3]. Recent improvements in stabilization of the output power based on monitoring the tissue impedance help to maintain constant cutting and coagulation rate in variable conditions at the electrode-tissue interface, but does not significantly change the extent of associated

thermal damage [3], [4]. Pulsed waveforms with variable duty cycle are used only for tissue coagulation [4].

Laser surgery started in the late 1960s with continuous waveform instruments, but unlike electrosurgery, the field of medical lasers has rapidly evolved. Higher and higher precision, lower collateral damage, and better targeting of specific tissue layers were achieved by optimizing laser wavelength, pulse duration, beam shape, and repetition rate. For example, the very common modern ophthalmic laser applications, such as photoablation of the cornea with ArF excimer laser (LASIK), or dissection of a corneal flap with ps Nd:YLF laser exhibit micrometer precision and sub-cellular width of the collateral damage zone.

In this letter, we demonstrate that sub-cellular precision can also be achieved with electrosurgery, if the mechanisms of interaction are understood and associated waveform parameters and electrode geometry are properly optimized.

## II. THEORETICAL CONSIDERATIONS

The basic mechanism of tissue ablation and dissection in electrosurgery involves Joule heating of the conductive tissue by electric current, that leads to vaporization and ionization of the water content in the tissue adjacent to the electrode, and ultimately to vapor expansion and tissue fragmentation [3], [4]. Tissue heated below the vaporization threshold remains in place, but can undergo thermal denaturation, with its extent determined by the temperature levels and duration of the hyperthermia. The depth of heat penetration into tissue is determined by the distribution of electric field (source of heating) and by thermal diffusion. Thus, to confine the collateral damage zone in tissue, both of these factors should be minimized.

### A. Penetration of Electric Field Into Tissue

The distribution of electric field is determined by electrodes geometry. Electric field around a spherical electrode having constant electric field on its surface scales with electrode radius  $r_o$  and distance  $r$  as  $E \propto (r_o/r)^2$ , and around a cylindrical electrode as  $E \propto r_o/r$ . For both configurations, the penetration depth of electric field in tissue is on the order of the electrode radius. Thus electrodes with a small radius of curvature should be used to minimize the affected zone of tissue. For example, to limit penetration of the electric field into tissue to cellular size ( $\approx 7 \mu\text{m}$ ), the electrode radius of curvature should not exceed similar dimensions. (Additional attenuation of the propagating electromagnetic radiation in tissue in the frequency range below 10 MHz is insignificant for our discussion. For example, penetration depth of the 20 MHz radiation in tissue is approximately 20 cm [5], while we are interested in confinement of electric field by micrometers.)

Manuscript received October 14, 2007. This work was supported in part by the NIH under Grant 2R01 EY012888-04 and by the Air Force Office of Scientific Research under MFEL Grant. D. Palanker and A. Vankov have patent disclosures related to the described technology which are assigned to Stanford University. These patents have been licensed by Stanford University Office of Technology Licensing to PEAK Surgical Inc. *Asterisk indicates corresponding author.*

\*D. V. Palanker is with the Department of Ophthalmology and Hansen Experimental Physics Laboratory, Stanford University, 452 Lomita Mall, Stanford, CA 94305-4085 USA (e-mail: palanker@stanford.edu).

A. Vankov is with the PEAK Surgical Inc., Palo Alto, CA 94303 USA.

P. Huie is with the Department of Ophthalmology and Hansen Experimental Physics Laboratory, Stanford University, Stanford, CA 94305-4085 USA.

Digital Object Identifier 10.1109/TBME.2007.914539

### B. Heat Diffusion

Penetration of heat into tissue by diffusion depends on pulse duration  $t$  as following:  $L = \sqrt{4kt}$ , where  $k$  is the thermal diffusivity of tissue [6]. An upper estimate of the heat penetration depth can be obtained assuming  $k$  being the heat diffusivity of water  $k = 1.4 \times 10^{-7} \text{ m}^2/\text{s}$ . To limit heat diffusion to cellular size  $L \approx 7 \mu\text{m}$ , the pulse duration  $t$  should not exceed  $100 \mu\text{s}$ . (Effect of blood perfusion on tissue temperature is negligible at exposure durations not exceeding 1 s [7]). In addition, if repetitive pulses are applied, heat accumulation should be prevented by providing sufficient delay between pulses for energy dissipation from the heated area.

### C. Cavitation

In pulsed ablation, tissue can also be damaged by mechanical effects of the rapidly expanding and collapsing cavitation bubbles [8], [9]. When the pulse duration is much shorter than the lifetime of the vapor bubble, the process of vaporization is explosive, leading to the formation of large and rapidly expanding vapor cavities. During collapse of the cavitation bubbles, fast water jets can form near the tissue boundaries, extending the range of mechanical tissue damage [9], [10]. With pulse duration much shorter than the bubble lifetime, up to 10% of the pulse energy can be converted into mechanical energy of the cavity [11], [12]. Pulse energy required for explosive vaporization of a surface water layer around a hemispherical electrode of radius  $r$  is [11]:  $E_{\text{th}} = 2\pi r^3 \rho C (T_{\text{max}} - T_0)$ , where  $\rho$  is tissue density,  $C$  is its specific heat capacity,  $T_0 = 37^\circ\text{C}$  is the starting temperature and  $T_{\text{max}}$  is the explosive vaporization threshold at the electrode-water interface, which varies between 200 and 300 °C depending on surface properties [13]. If a fraction  $f$  of this energy is converted into a vapor cavity (with its mechanical energy  $E_{\text{bub}} = P \cdot V$ ), its radius will be  $R = r \cdot (3f * \rho C \Delta T / P)^{1/3}$ , where  $P$  is the pressure in the liquid and  $V$  is the volume of a hemispherical cavity at maximal expansion. For  $f = 10\%$ , atmospheric pressure  $P$  and  $T_{\text{max}} = 200^\circ\text{C}$ , the  $R \approx r * 13$ . Thus, for  $r = 7 \mu\text{m}$ ,  $R = 89 \mu\text{m}$ . Lifetime of the spherical vapor cavity [14]:  $\tau = 0.91R\sqrt{\rho/P} \approx 8 \mu\text{s}$  in our case. Thus, mechanical damage associated with cavitation can be prevented if the pulse duration will exceed a few microseconds.

### D. Electroporation

Another potentially damaging mechanism of interaction in electrosurgery is the direct effect of electric field on cellular membranes. Due to polarization of the cell in an electric field, its transmembrane potential is increased on the anodic side (hyperpolarization) and decreased on the cathodic side (depolarization) [15]. Depolarization of the cellular membrane by a few millivolts can cause opening of the voltage-sensitive ion channels leading to stimulation of the neural and muscle cells. When the trans-membrane voltage reaches a level of approximately 1 V the lipid bilayer starts breaking up forming hydrophilic pores. This effect, called electroporation, is utilized for delivery of macromolecules in and out of cells [15]. The trans-membrane voltage increases with time  $t$  as  $\Delta V \propto 1 - \exp(-t/t_p)$ , where cellular polarization time  $t_p = a * C_m * (\gamma_i + \gamma_e/2)$  [16]. At pulse durations  $t < t_p$  this dependence can be approximated

as  $\Delta V \propto t/t_p$ . With cell diameter  $a = 7 \mu\text{m}$ , membrane capacitance per unit area  $C_m \approx 1 \mu\text{C}/\text{cm}^2$ , intracellular medium resistivity  $\gamma_i = 220 \Omega \cdot \text{cm}$ , and extracellular medium resistivity  $\gamma_e$  in the range of 100 to 1000  $\Omega \cdot \text{cm}$ , the cellular polarization time  $t_p = 0.19 - 5 \mu\text{s}$  [16]. The cell is fully polarized at pulse durations  $t \gg t_p$ . After full polarization, the threshold of electroporation scales with pulse duration as  $t^{-1/2}$  due to dynamics of the pore formation [17]. Since both of these processes, cellular polarization, and pore formation, are minimized with decreasing pulse duration  $t$ , the electroporation-related damage can be minimized by the use of bursts of shorter pulses of alternating polarity. Threshold of electroporation increases with decreasing pulse duration especially rapidly ( $E \propto t^{-3/2}$ ) when pulses shorter than the cellular polarization time ( $t < t_p$ ) are applied.

Thus, in summary, for pulsed electrosurgery with cellular precision the radius of curvature of the electrode should not exceed cellular size. Burst duration should be selected such that it allows for prevention of both, mechanical damage due to vigorous cavitation on the short end, and thermal diffusion on the long end. For the electrode with radius of curvature equal to  $7 \mu\text{m}$ , burst duration should be in the range of 5 to  $100 \mu\text{s}$ . To minimize electroporation and muscle activation, duration of a half-cycle within the burst should not exceed the cellular polarization time, so for  $t_p = 200 \text{ ns}$  the frequency should exceed 2.5 MHz.

## III. EXPERIMENTAL RESULTS AND DISCUSSION

To dissect tissue to an arbitrary depth, an elongated electrode is required. A wire electrode with diameter of a few micrometers is impractical due to its extreme flexibility and poor visibility. We have developed a  $12 \mu\text{m}$  thin foil electrode with insulated sides and exposed edge. Flat sides of the electrode are coated with glass, as shown in Fig. 1(a)–(d), leaving only the semi-cylindrical edge of the foil having radius of curvature of  $6 \mu\text{m}$  exposed to the conductive physiological medium. Very thin insulation ( $10 \mu\text{m}$ ) does not obstruct insertion of the electrode into the tissue during cutting.

Dimensions of the blade electrodes can be adjusted for different applications. For example, the typical size for general surgery is 10 mm in length and 5 mm in width. In neurosurgical applications smaller blades are required—about 5 mm in length and 3 mm in width. Intraocular applications require even smaller dimensions—1 mm in length and 0.6 mm in width. Due to the small size of the exposed part of the active electrode its performance is practically independent on the location and size of the larger return electrode. It works equally well with a local (bipolar configuration) or a remote return electrode (monopolar configuration). The impedance of the discharge zone is determined by the size of the small active electrode, and electric field is concentrated around it. Thus, placement of the return electrode is determined only by considerations of surgical convenience. For example, monopolar geometry with a remote pad electrode is suitable for dermal applications, while for intraocular surgery a coaxial return electrode is more appropriate.

We designed and built a pulse generator that provides square wave constant voltage waveform with active switching between the symmetric positive and negative bias levels with a transition time of 15 ns at pulse frequency of 4 MHz. To avoid any

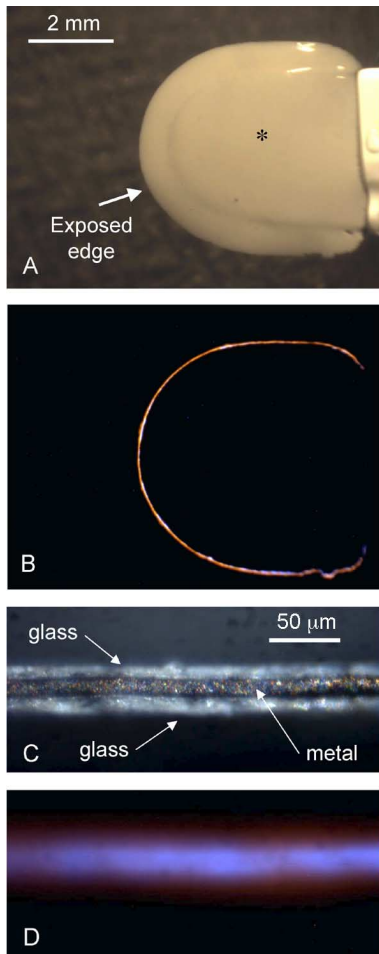


Fig. 1. (a) Front view of the blade electrode with insulated sides and exposed edge. Thicker central part of the blade (indicated by \*) enhances rigidity. Scale bar is 2 mm. (b) Plasma discharge along the exposed edge. (c) High magnification side view of the blade demonstrating 12.5  $\mu\text{m}$  edge of the metal foil and 10  $\mu\text{m}$  layers of glass insulation. (d) Plasma discharge along the metal edge extending by approximately twice the width of the electrode.

non-compensated charge injection into tissue the output of the pulse generator is connected to the electrode via a 10 nF capacitor. Typical waveforms of voltage, current, and light emission obtained on a blade with a perimeter of 8 mm are shown in Fig. 2. The first 6  $\mu\text{s}$  correspond to the water heating phase, when the current amplitude remains practically constant. Upon beginning of vaporization part of the electrode surface becomes covered with a non-conductive layer of vapor, leading to an increase in impedance, and a corresponding decrease in electric current, as seen in the plot between 6 and 12  $\mu\text{s}$ . When the vapor cavity is ionized and conductivity through the vapor cavity is restored, the current and impedance stabilize. This plasma-mediated discharge begins after 11  $\mu\text{s}$ , and is maintained until the end of the burst, as shown in Fig. 2. The burst energy at these settings is 13 mJ and average power during the burst is 765 W. At a burst repetition rate of 100 Hz, the duty cycle is 0.17% and the average power is 1.3 W.

Since tissue ejection occurs at temperatures exceeding the water boiling temperature [18], ionization of the water vapor is essential for continuing energy deposition into the tissue above the vaporization threshold. Without ionization, the water vapor

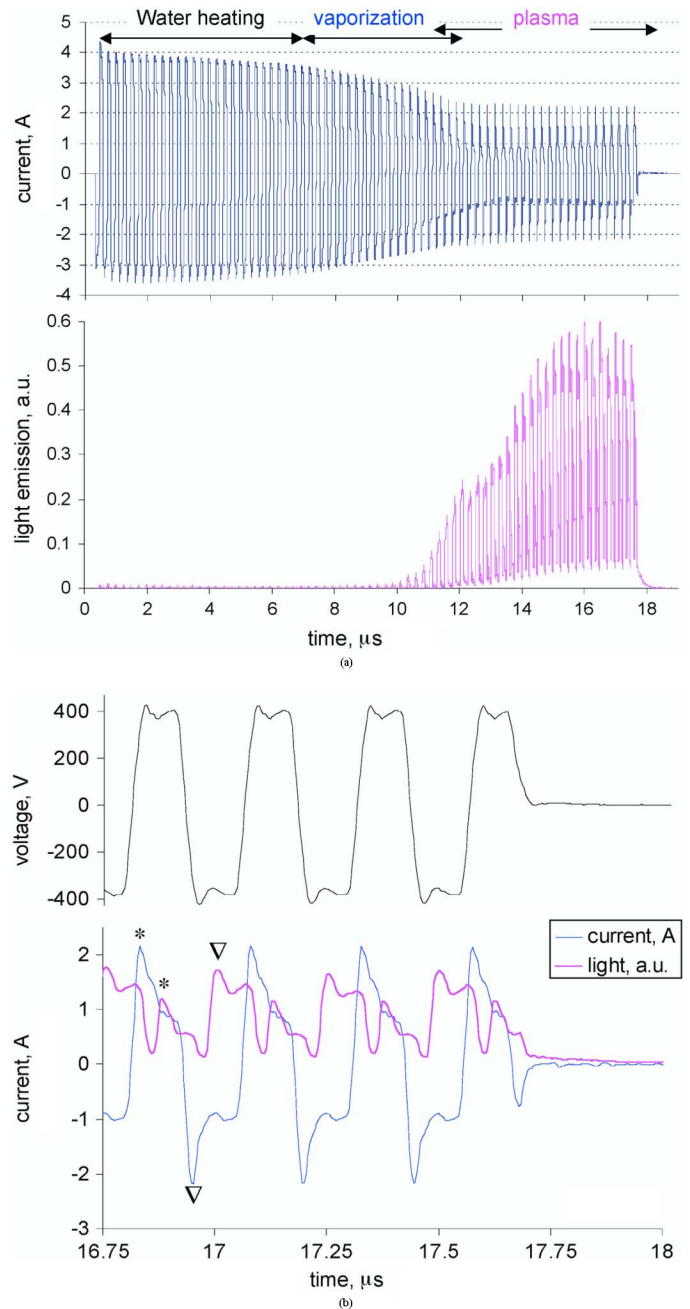


Fig. 2. (a) Waveforms of the current and light emission during the burst. Phases of water heating, vaporization, and ionization are shown by the arrows. (b) Voltage, current, and light emission by the plasma during the last microsecond of the burst. Note a 50 ns delay between the peaks of current and light emission, and the lower brightness during the positive phase (\*).

would isolate the electrode and prevent further energy flow and associated heating.

Total energy deposited during the burst can be controlled by adjusting the voltage amplitude and burst duration. Ionization threshold of the water vapor is approximately  $-200$  V and  $+400$  V in the negative and positive polarities, respectively [12]. To support plasma generation in both alternating polarities the output voltage level was maintained above  $\pm 400$  V. Optimal duration of the burst for each electrode depends on tissue type: duration of the plasma-mediated phase of the discharge

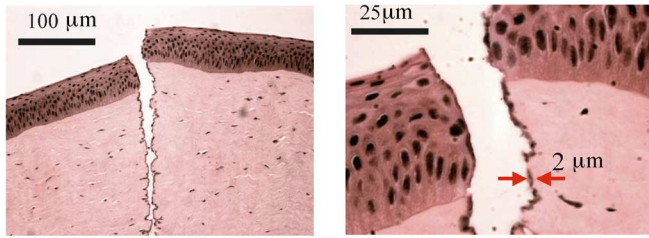


Fig. 3. Histological section of a cut produced in a fresh porcine cornea *in vitro*. Note that the width of the thermal damage zone (darkened area at the edges of the lesion) does not exceed  $2\ \mu\text{m}$ .

can vary from a few microseconds in very soft tissues to a few tens of microseconds in tougher tissues, such as tendon and skin. The cutting speed can be adjusted by varying the burst repetition rate. For example, optimal settings for cutting porcine skin at a linear speed of 10 mm/s are as follows: amplitude  $\pm 450\ \text{V}$ , burst duration  $38\ \mu\text{s}$  (150 cycles), repetition rate up to 500 Hz. Dissection of porcine cornea with a linear speed of 2 mm/s was achieved at the following settings: 400 V,  $38\ \mu\text{s}$ , 100 Hz. Pulse energy in this regime is 22 mJ, duty cycle is 0.38%, and average power is 2.2 W. Cutting speed of 2 mm/s at repetition rate of 100 Hz corresponds to an ablation rate of  $20\ \mu\text{m}$  per pulse. Assuming the width of the ablated zone is similar to its depth (cylindrical symmetry), the pulse energy of 2.75 mJ per mm length of the cutting edge corresponds to volumetric energy density of ablation  $\approx 6.8\ \text{kJ}/\text{cm}^3$  or ablation efficiency of  $147\ \mu\text{g}/\text{J}$ . This value is remarkably similar to the maximal ablation efficiency of pulsed lasers in the “blow-off” model  $-145\ \mu\text{g}/\text{J}$  [18, Fig. 3(a)], and is very close to typical experimental values for ArF excimer laser ablation of the cornea  $\approx 150\ \mu\text{g}/\text{J}$  [6, Fig. 3.36].

Histology of a cut in fresh porcine cornea, shown in Fig. 3, demonstrates very clean and sharp edges of the incision. The thermal damage zone extends only  $2\ \mu\text{m}$  in both the collagenous stroma and the epithelial cell layer. Similar results have been achieved in porcine skin.

Due to almost complete coverage of the electrode with insulator, leaving only a thin edge exposed, such electrodes operate equally well in both dry and wet fields, i.e., immersed in conductive medium or at the air-tissue interface. Such universality is especially important in applications where the amount of fluid in the field can change during the operation. Examples of such “dual” mode applications include arthroscopy, ENT, neurosurgery, and ophthalmology. The traction-free nature of electrosurgical cutting allows for non-deforming dissection of tough tissues such as cartilage, tendon, and skin, as well as flimsy membranes, such as the ocular lens capsule and vitreoretinal membranes.

Removal of bulk tissue in our approach can be performed by excision of tissue blocks rather than by layered vaporization. For example, a cheese cutter-shaped electrode with insulated planar sides and exposed cutting edge that generates a layer of plasma allows for traction-free excision of tissue slices.

In summary, we have demonstrated that pulsed electrosurgery with properly optimized microelectrodes and microsecond elec-

trical waveforms can provide sub-cellular precision in tissue dissection, which can rival many advanced lasers. The greatly reduced zone of thermal damage with our instrument, as compared to conventional continuous RF electrosurgery, will provide faster healing and less scarring. It will allow for higher precision of tissue manipulation, and thus enable more delicate procedures. Universal applicability of the probes for dry and wet fields will simplify surgical procedures by eliminating the need for changing instruments during various surgical maneuvers.

#### ACKNOWLEDGMENT

The authors would like to thank R. Dalal for the histological preparations and photography.

#### REFERENCES

- [1] S. V. Pollack, A. Carruthers, and R. C. Grekin, “The history of electro-surgery,” *Dermatologic Surgery*, vol. 26, pp. 904–908, 2000.
- [2] W. T. Bovie, “New electro-surgical unit with preliminary note on new surgical-current generator,” *Surg. Gynecol. Obstet.*, vol. 47, pp. 751–752, 1928.
- [3] D. B. Brown, “Concepts, considerations, and concerns on the cutting edge of radiofrequency ablation,” *J. Vasc. Interventional Radiol.*, vol. 16, pp. 597–613, 2005.
- [4] N. N. Massarweh, N. Cosgriff, and D. P. Slakey, “Electrosurgery: History, principles, and current and future uses,” *J. Amer. College Surgeons*, vol. 202, pp. 520–530, 2006.
- [5] P. A. Bottomley and E. R. Andrew, “RF magnetic-field penetration, phase-shift and power dissipation in biological tissue - implications for NMR imaging,” *Phys. Med. Biol.*, vol. 23, pp. 630–643, 1978.
- [6] M. Niemz, *Laser-Tissue Interactions. Fundamentals and Applications*. Berlin, Germany: Springer, 2002.
- [7] J. Kandulla, H. Elsner, R. Birngruber, and R. Brinkmann, “Noninvasive optoacoustic online retinal temperature determination during continuous-wave laser irradiation,” *J. Biomed. Opt.*, vol. 11, pp. 1–13, 2006.
- [8] J. M. Miller, D. V. Palanker, A. Vankov, M. F. Marmor, and M. S. Blumenkranz, “Precision and safety of the pulsed electron avalanche knife in vitreoretinal surgery,” *Archives Ophthalmology*, vol. 121, pp. 871–877, 2003.
- [9] D. Palanker, A. Vankov, J. Miller, M. Friedman, and M. Strauss, “Prevention of tissue damage by water jet during cavitation,” *J. Applied Phys.*, vol. 94, pp. 2654–2661, 2003.
- [10] D. V. Palanker, M. F. Marmor, A. Branco, P. Huie, J. M. Miller, S. R. Sanislo, A. Vankov, and M. S. Blumenkranz, “Effects of the pulsed electron avalanche knife on retinal tissue,” *Arch. Ophthalmol.*, vol. 120, pp. 636–40, 2002.
- [11] D. Palanker, I. Turovets, and A. Lewis, “Electrical alternative to pulsed fiber-delivered lasers in microsurgery,” *J. Appl. Phys.*, vol. 81, pp. 7673–7680, 1997.
- [12] A. Vankov and D. Palanker, “Nanosecond plasma-mediated electrosurgery with elongated electrodes,” *J. Appl. Phys.*, vol. 101, p. 124701, 2007.
- [13] O. C. Thomas, R. E. Cavicchi, and M. J. Tarlov, “Effect of surface wettability on fast transient microboiling behavior,” *Langmuir*, vol. 19, pp. 6168–6177, 2003.
- [14] F. R. Young, *Cavitation*. New York: McGraw-Hill, 1989, pp. 13–16.
- [15] J. C. Weaver and Y. A. Chizmadzhev, “Theory of electroporation: A review,” *Bioelectrochem. Bioenergetics*, vol. 41, pp. 135–160, 1996.
- [16] M. Hibino, H. Itoh, and K. Kinosita, “Time courses of cell electroporation as revealed by submicrosecond imaging of transmembrane potential,” *Biophys. J.*, vol. 64, pp. 1789–1800, 1993.
- [17] R. P. Joshi and K. H. Schoenbach, “Electroporation dynamics in biological cells subjected to ultrafast electrical pulses: A numerical study,” *Phys. Rev. E*, vol. 62, pp. 1025–1033, 2000.
- [18] A. Vogel and V. Venugopalan, “Mechanisms of pulsed laser ablation of biological tissues,” *Chem. Rev.*, vol. 103, p. 577, 2003.